European Journal of Radiology 188 (2025) 112154

Contents lists available at ScienceDirect

European Journal of Radiology

journal homepage: www.elsevier.com/locate/ejrad

Ultra-high resolution photon-counting detector coronary CT minimizes overestimation bias compared to invasive reference

Gerald Siegfried Laux [a,1], Moritz C. Halfmann [b,1], Larissa Kavermann [a], Stefanie Bockius [b], Maike Knorr [a], Tommaso Gori [a], Pal Maurovich-Horvat [d], Akos Varga-Szemes [c], Philipp Lurz [a], Tobias Bäuerle [b], Michaela M. Hell [a,*,1], Tilman Emrich [a,c,1]

[a] Department of Cardiology, University Medical Center of the Johannes Gutenberg-University, Mainz, Germany
[b] Department of Diagnostic and Interventional Radiology, University Medical Center of the Johannes Gutenberg-University, Mainz, Germany
[c] Division of Cardiovascular Imaging, Department of Radiology and Radiological Science, Medical University of South Carolina, Charleston, United States
[d] Department of Radiology, Medical Imaging Center, Semmelweis University, Budapest, Hungary

ARTICLE INFO

Keywords:
Coronary artery disease
photon-counting detector CT
Ultrahigh-resolution
Coronary computed tomography angiography
Quantitative coronary angiography

ABSTRACT

Background: Photon-counting detector (PCD) coronary CT angiography (CCTA) at ultra-high-resolution (UHR) is a promising tool for the detailed evaluation of the coronary arteries. However, correlation with invasive quantitative coronary angiography (QCA) has not been thoroughly investigated. We here evaluated the efficacy of UHR-CCTA against invasive QCA in patients suspected of coronary artery disease (CAD).
Methods: Retrospectively, patients suggestive of CAD were included if they had undergone UHR-CCTA on a PCD-CT system showing coronary stenosis which clinically indicated subsequent invasive coronary angiography and no prior coronary interventions. CCTA datasets were reconstructed in 0.6 mm, 0.4 mm, and UHR 0.2 mm slice thicknesses. The extent of stenosis was compared between QCA and CCTA using univariate analysis of variance with post-hoc testing and Bland-Altman plots. Diagnostic performance was assessed based on the detection of relevant coronary stenosis (≥50 %) as confirmed by QCA.
Results: Forty-nine patients (71 ± 9 years; 37 % male) were included. Stenosis evaluation for 103 segments revealed decreasing mean stenosis diameter with improving spatial resolution (61.4 % for 0.6 mm, 55.3 % for 0.4 mm, 50.9 % for UHR 0.2 mm; $p \leq 0.001$). Bias between CCTA and QCA decreased with increasing resolution (13.2 %, limits of agreement [LoA] 30 vs. 9.4 %, 28.1 vs. 5.2 %, 23). UHR-CCTA reconstructions showed superior diagnostic accuracy and positive predictive value (PPV) for detecting relevant CAD compared to lower resolutions (61.2 vs. 61.2 % vs. 71.4 and 53.7 % vs. 53.9 vs. 61.8 %, respectively).
Conclusions: UHR-CCTA with photon-counting detector CT demonstrated a decrease in overestimation bias and an increase in PPV.

Short summary

Photon-counting detector CT with ultra-high-resolution (UHR) mode shows promise in enhancing coronary assessment by offering higher spatial resolution. In the present study, UHR- coronary CT angiography (CCTA) was compared to invasive quantitative coronary angiography (QCA) for evaluating coronary stenosis. Results revealed that UHR-CCTA significantly reduces overestimation bias in stenosis measurements, particularly in heavily calcified plaques, a known limitation of previous imaging methods. This advancement improves the accuracy of

Abbreviations: CAD, Coronary artery disease; CAD-RADS, Coronary artery disease reporting and data system; CCTA, Coronary CT angiography; EID, Energy-integrating detector; HR, High resolution; ICA, Invasive coronary angiography; LoA, Lower limits of agreement; NPV, Negative predictive value; PCD-CT, Photon-counting detector computed tomography; QCA, Quantitative coronary angiography; SCCT, Society of Cardiovascular Computed Tomography; SR, Standard Resolution; UHR, Ultra-high resolution.

* Corresponding author at: Department of Cardiology, University Medical Center of the Johannes Gutenberg-University, Langenbeckstraße 1, Mainz 55131, Germany.
E-mail address: Michaela.Hell@unimedizin-mainz.de (M.M. Hell).
[1] These authors contributed equally.

https://doi.org/10.1016/j.ejrad.2025.112154
Received 3 March 2025; Received in revised form 16 April 2025; Accepted 30 April 2025
Available online 6 May 2025

coronary CT angiography, may reduce unnecessary diagnostic procedures and potentially impacting clinical practice for patients with suspected coronary artery disease.

1. Introduction

Coronary CT angiography (CCTA) has been shown to be highly effective in excluding coronary artery disease (CAD) in patients with a low to intermediate pretest probability for CAD [1–3]. The significance of diagnostic tools that deliver high accuracy for making informed decisions in the management of suspected CAD cannot be overstated, considering the substantial morbidity and mortality associated with this condition [1]. Diagnostic information of conventional CCTA is affected by substantial calcifications, which can introduce inaccuracies in characterizing luminal stenosis, leading to an overestimation of stenosis severity [4].

Emerging technological innovations, such as photon-counting detector CT (PCD-CT), help limit such disadvantages compared to conventional energy-integrating detector (EID) CT systems [5]. Enhanced resolution inherent in PCD-CT resulting from its smaller detector element size and direct transformation of x-ray photons into electrical signal allow for an ultra-high resolution (UHR) acquisition mode with maximum in-plane and through-plane resolutions of 0.11 mm and 0.16 mm [6]. Recent preliminary findings have demonstrated the feasibility of UHR-CCTA for detecting CAD in a high-risk population [7]. Nevertheless, evidence regarding quantitative stenosis assessment using UHR-CCTA compared with invasive quantitative coronary angiography (QCA) reference is scarce.

The aim of this study was to evaluate the efficacy of UHR-CCTA against invasive QCA in patients suspected of CAD.

2. Materials and methods

2.1. Patient population

The institutional database between June 2022 and July 2023 was retrospectively reviewed, and patients were included if they met the following criteria: I) UHR-CCTA due to symptoms suspicious of CAD or clinically suspected progression of known CAD, performed on a PCD-CT system; II) Subsequent clinically indicated invasive coronary angiography (ICA) within 30 days; III) stenosis category CAD-RADS (coronary artery disease reporting and data system) 3 or higher on CCTA; and IV) 18 years of age or above. Patients were excluded from the subsequent analysis if either their CCTA or QCA results were considered non-diagnostic by a board-certified radiologist or cardiologist, or if they had pre-existing coronary stents before undergoing the CCTA (Fig. 1). Covariates, including cardiac history and risk factors, were extracted from the patients' medical records. The local ethics committee approved the protocol of this single –center retrospective study with waivers of informed consent (reference number 2022–16359).

2.2. CCTA image acquisition

CCTA scans were performed with a PCD-CT system (NAETOM Alpha, version VA50, Siemens Healthineers, Forchheim, Germany, gantry rotation time 0.25 s) according to institutional standard operating protocols. After a non-contrast scan for coronary artery calcium scoring, the clinical decision to perform CCTA in UHR mode (tube voltage 120 kVp with a vendor-specific automated image quality level set at 60) with a slice thickness of 0.2 mm was guided by an Agatston-score threshold of $\geq$ 10. Before scanning, patients received sublingual nitrates (0.4 mg) and intravenous metoprolol (up to 20 mg) based on heart rate and absence of contraindications. A test-bolus acquisition for optimal bolus-timing was applied. For contrast media, an automated dual-cylinder pump was utilized, which provided a flow rate of 4 ml/s over two injection phases of 70 ml iodinated contrast agent (iopromide, 370 mgI/ml) and 25 ml of saline flush.

Depending on the patient's heart rate and variability, CCTA was either acquired in sequential scan mode with prospective ECG-gating at end-diastole, a broadened acquisition window at end-diastole, or in spiral acquisition mode with retrospective ECG-gating. Metoprolol was administered to patients with heart rates exceeding 70 beats per minute to facilitate prospective scanning whenever possible. Image reconstructions included three different slice thicknesses of 0.6 mm (mimicking a conventional EID-CT standard resolution (SR)), 0.4 mm (high resolution (HR)), and 0.2 mm (UHR), as described before [8]. Vascular reconstruction kernels were applied (0.6/0.4 mm: Bv44 and 0.2 mm: Bv64). The effective radiation dose was calculated using a cardiac-specific conversion factor of 0.026 mSv/(mGy $\times$ cm) [9].

2.3. ICA image acquisition

Patients with CCTA-suspected significant CAD, defined as at least one coronary stenosis with luminal narrowing exceeding 50 % (CAD-

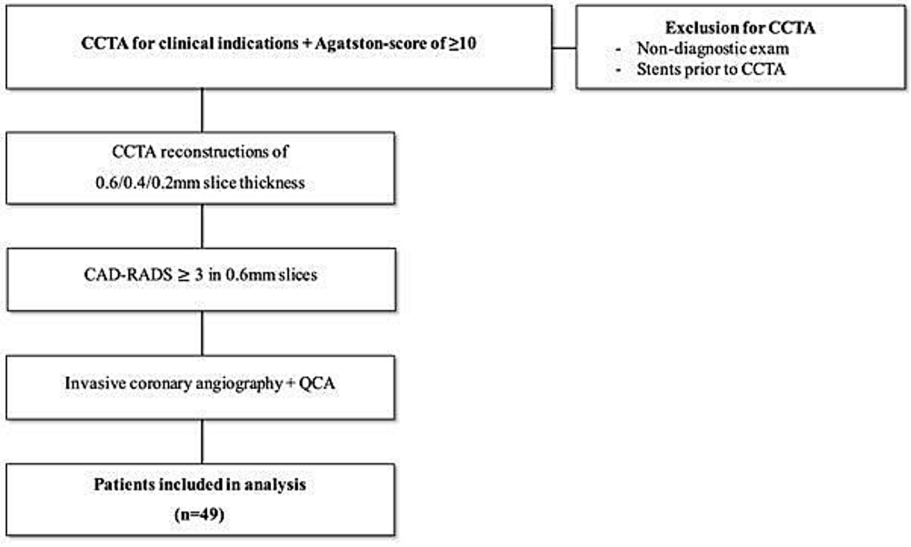

Fig. 1. Patient inclusion and exclusion flowchart. CAD-RADS, Coronary Artery Disease Reporting and Data System, CCTA, Coronary CT angiography, QCA, Quantitative Coronary angiography.

RADS ≥ 3) were discussed in an interdisciplinary meeting between a board-certified cardiologist and radiologist. The decision for further stenosis evaluation with either ischemia testing or directly proceeding to ICA was made following current international guidelines [1]. All ICA examinations were performed according to institutional standard operating procedures by board-certified interventional cardiologists on a fluoroscopy system (Allura Xper FD10, Philips Healthcare, Best, The Netherlands).

2.4. Stenosis assessment in UHR CCTA and QCA

Grading of coronary stenoses from both CCTA and QCA was based on the quantification of the smallest diameter within the stenosis (D_s) in relationship to the expected vessel diameter at the site of stenosis (D_{ref}). The expected vessel size was interpolated from a proximal and distal reference site, taking anatomical tapering of the vessels into account [10]. The following equation was used for stenosis quantification:

$$(\text{Minimal lumen diameter } (D_s)/\text{Reference diameter } (D_{ref})) \times 100 \quad [11]$$

Segments with chronic total occlusion were excluded from the analysis. Coronary segments 1, 2, 5–7, 11–13, and 17 were categorized as proximal, the other segments as distal [11]. Plaques were classified as calcified, partially calcified, and non-calcified according to current terminology [12]. For stenosis assessment of CCTA, two blinded readers (M.C.H. and S.B. with 5 and 2 years of experience in CCTA, respectively) quantified coronary stenoses using a dedicated semi-automatic post-processing software (Syngo.via, version VB50A HF3, Siemens Healthineers).

For ICA stenosis assessment, two blinded readers (with 2 and 6 years of experience in invasive cardiology) were provided with the coronary segments with luminal narrowing ≥ 50 % in CCTA to guide QCA analysis. The readers were blinded to quantitative CCTA results to minimize confirmation bias. If multiple ICAs were performed within 30 days after CCTA for a patient, the ICA closest in time to the CCTA was selected. QCA was performed using a dedicated software (CAAS Workstation 8.5, Pie Medical Imaging B.V., Maastricht, The Netherlands) according to latest recommendations [13]. Particular attention was drawn on minimizing vessel motion and ensuring optimal contrast agent filling of the vessel. When required, manual tracing was performed for obstruction length and reference diameter [13]. After performing QCA, the stenosis measurement with the highest degree of luminal narrowing per segment was reported and utilized for analysis. Board-certified cardiologists and radiologists independently reviewed cases with inconsistencies between CCTA and ICA results regarding stenosis location [11].

2.5. Statistical analysis

All statistical analyses were performed using dedicated software (SPSS for Windows; version 23.0; IBM Corporation, Armonk, NY, USA). Shapiro-Wilk tests were used to test continuous variables for normality of distribution. Results are reported as mean ± standard deviation or median with inter-quartile ranges (IQR, Q1, Q3). Categorical variables are reported as absolute frequencies with respective proportions (%). Differences between quantitative results of CCTA and QCA were compared using Bland-Altman analysis (absolute mean bias and respective upper and lower limits of agreement (LoA), defined as 1.96 × standard deviation of bias). The results were compared between the three CCTA reconstructions and QCA by the Wilcoxon related samples signed rank test with Bonferroni correction (0.05/4 = 0.013). Agreement between radiologist and cardiologist readers was evaluated separately by using two-way random-effects model intraclass correlation coefficients (ICC). Levels of agreement were defined as follows: poor, <0.5; moderate, 0.5–0.75; strong, 0.76–0.9; excellent, >0.9 [14]. Those were calculated based on plaque type and differentiation between proximal and distal segments. Receiver operating characteristic curve analysis was conducted, along with the calculation of the area under the curve (AUC), to assess the diagnostic performance of SR, HR, and UHR CCTA in comparison with the reference standard ICA. Sensitivity, specificity, positive predictive value (PPV), negative predictive value (NPV), and accuracy were calculated for both stenoses ≥ 50 % and ≥ 70 % on CCTA based on per-patient, per-vessel and per-segment levels, as well as for left and right coronary arteries. Statistical significance was set as $p < 0.05$.

3. Results

3.1. Patient and coronary imaging characteristics

Out of 51 patients referred for CCTA, two patients were excluded from subsequent analysis because either their CCTA or QCA was deemed non-diagnostic. Ultimately, the study cohort comprised 49 patients (63 % females, mean age 71 ± 9 years). Median time gap between CCTA and ICA was 8 (1.5, 25.5) days. A retrospectively gated spiral acquisition or extended triggering window were applied in 8 % of patients. Mean heart rate was 65 ± 9 beats per minute and the median Agatston score was 993 (407, 2137). Patient characteristics and CCTA acquisition parameters are reported in Tables 1 and 2.

3.2. CCTA stenosis assessment

Among the total of 882 coronary segments evaluated, 8 segments were excluded due to chronic total occlusions. Among the remaining 874 analyzed coronary segments, stenosis quantification based on SR reconstructions suggested 245 (28 %) of segments with relevant stenosis (diameter stenosis ≥ 50 %) while HR (222, 25 %) and UHR (174, 20 %) reconstructions suggested a lower prevalence. The stenoses were predominantly caused by calcified plaques (70 %), followed by partially calcified (19 %) and non-calcified plaques (11 %). The majority of stenoses were found in the proximal segments (73 %) (Table 3). The median degree of diameter stenosis continuously decreased with increasing spatial resolution (SR 61.4 (50.9, 70.8) % vs. HR 55.3 (46.4, 67.8) % vs. UHR 50.9 (42.9, 63.1) %, all $p < 0.001$, Fig. 2). A significant decline in diameter stenosis with increasing spatial resolution was confirmed for both proximal and distal coronary segments (Table 3). When categorized by plaque type, a significant reduction in stenosis diameter with increasing resolution was evident only for calcified plaques (Table 4). No significant reduction in stenosis diameter was found for non-calcified or partially calcified plaques. However, a significant decrease in diameter stenosis from SR to HR in partially calcified plaques was found.

Table 1
Patient Characteristics.

	(n = 49)
Age, years	70.8 ± 8.7
Female	31 (63 %)
BMI, kg/m^2	27.2 (24.8, 31.2)
≥ 25 kg/m^2	17 (35 %)
≥ 30 kg/m^2	16 (33 %)
Cardiovascular risk factors	
Dyslipidemia	31 (63 %)
Arterial hypertension	42 (86 %)
Diabetes mellitus	8 (16 %)
Family history of CAD[a]	3 (6 %)
Tobacco use	15 (31 %)

Values are mean ± SD, n (%), or median (IQR), unless otherwise indicated.
BMI, body mass index; CAD, coronary artery disease; CCTA, coronary computed tomography angiography.
[a] Defined as family history of CAD in a male first-degree relative before age 55 or in a female first-degree relative before age 65.

Table 2
Imaging characteristics based on CCTA.

CCTA	n = 49
Tube voltage, kVp	120
Gating technique	
Sequential	45 (92 %)
Retrospective spiral	4 (8 %)
Preparation and basic information	
Nitroglycerine	49 (100 %)
Metoprolol	38 (78 %)
Heart rate, 1/min	65 ± 9
Atrial fibrillation at scan	4 (8 %)
Radiation dose, mSv	3.9 (3.2, 6.7)
CTDI, mGy	10.9 (9.0, 14.9)
DLP, mGycm	151.0 (124.0, 256.5)
Agatston score	993.0 (407.0, 2137.0)
Time between CCTA and QCA, days	8.0 (1.5, 25.5)
Coronary artery disease[a]	
Proximal[b] stenosis	32 (68 %)
Right coronary artery	9/32 (28 %)
Left anterior descending	11/32 (34 %)
Left circumflex	12/32 (38 %)
Distal stenosis	15 (32 %)
Right coronary artery	11/15 (73 %)
Left anterior descending	4/15 (27 %)

Values are mean ± SD, n (%), or median (IQR), unless otherwise indicated. CCTA, coronary computed tomography angiography; kVp, peak kilovolts; QCA, quantitative coronary angiography; CAD, coronary artery disease.
[a] Defined as luminal diameter stenosis ≥ 50 %in QCA assessment.
[b] Defined as coronary segments 1–2, 5–7, 11–13 and 17.

Table 3
Comparison of Stenosis Quantification.

		Bland-Altman			
all segments, n = 103[a]	Diameter stenosis	Bias	LoA	ICC	*P* value[b]
CCTA analysis					
SR	61.4 (50.9, 70.8)	13.2	30.0	0.72	<0.001
HR	55.3 (46.4, 67.8)	9.4	28.1	0.76	<0.001
UHR	50.9 (42.9, 63.1)	5.2	23.0	0.86	<0.001
QCA reference	46.4 (33.7, 59.8)	n/a			
proximal[c] segments, n = 75					
CCTA analysis					
SR	60.7 (50.5, 70.9)	13.0	31.9	0.71	<0.001
HR	52.8 (46.4, 69.0)	9.1	30.3	0.75	<0.001
UHR	50.0 (42.0, 64.7)	4.9	25.0	0.85	0.004
QCA reference	45.2 (30.9, 62.5)	n/a			
distal segments, n = 28					
CCTA analysis					
SR	64.7 (55.2, 71.0)	13.9	24.1	0.75	<0.001
HR	56.0 (52.0, 67.0)	10.1	20.4	0.82	<0.001
UHR	51.8 (47.1, 60.5)	6.0	15.8	0.90	0.003
QCA reference	48.4 (36.3, 56.5)	n/a			

LoA, Limits of agreement (1.96 × standard deviation of bias); ICC, intraclass correlation coefficient; CCTA, coronary computed tomography angiography; SR, standard resolution (0.6 mm slice thickness); HR, high resolution (0.4 mm); UHR, ultra-high resolution (0.2 mm); QCA, quantitative coronary angiography CAD, coronary artery disease.
[a] Number of coronary segments with QCA reference. For CCTA analysis, 1 distal segment was deemed non-assessable.
[b] Derived from non-parametric pairwise comparison to QCA reference.
[c] Defined as coronary segments 1–2, 5–7, 11–13 and 17.

Detailed results of comparison of stenosis quantification are summarized in Tables 3, 4 **and** S1.

3.3. Diagnostic performance of CCTA versus QCA

In comparison to QCA, Bland-Altman analyses (Fig. 3) showed decreasing overestimation bias (SR: 13.2 % vs. HR: 9.4 % vs. UHR: 5.2 %) and LoA (SR: 30.0 vs. HR: 28.1 vs. UHR: 23.0) of the diameter stenosis with increasing spatial resolution. Consequently, an increase in ICC could be observed with a strong level of agreement for UHR (ICC = 0.86). This was also evident for the subdivision into proximal and distal segments. Among the reconstructions, UHR showed the closest agreement of median diameter stenosis compared to QCA, but still with a significant difference (50.9 (42.9, 63.1)% vs. 46.4 (33.7, 59.8)%, p < 0.001). Detailed results of the stenosis assessment are summarized in Table 3. When split by plaque types (Table 4**,** Fig. 2), these results were only confirmed for calcified plaques and UHR. No difference was observed in non-calcified plaques between SR, HR and UHR compared to QCA. In partially calcified plaques, a significant difference between SR and QCA (62.4 (56.5, 68.4)% vs. 48.1 (37.9, 64.8)%, p = 0.017) and UHR and QCA (60.4 (49.6, 71.2)% vs. 48.1 (37.9, 64.8)%, p = 0.017) was found, but not for HR and QCA. Further, similar degrees of overestimation mean bias and LoA were found for non-calcified (SR: 3.3 % (20.9) vs. HR: 3.9 % (20.5) vs. UHR: 4.8 % (19.5)) and partially calcified plaque stenoses (SR: 9.8 % (31.0) vs. HR: 6.8 % (30.4) vs. UHR: 8.4 % (23.2)), while calcified plaque stenoses showed smaller mean bias and LoA for higher spatial resolutions (SR: 15.8 % (29.6) vs. HR: 11 % (28.2) vs. UHR: 4.3 % (23.5), Table 4).

UHR reconstructions led to the highest level of specificity on a per-patient basis in the identification of QCA stenosis ≥ 50 % (SR: 29.6 % vs. HR: 33.3 % vs. UHR: 51.6 %) as well as ≥ 70 % (SR: 61 % vs. HR: 68.3 % vs. UHR: 80.5 %, Fig. 4). Similarly, the PPV for stenosis detection differed among SR, HR and UHR reconstructions, with higher spatial resolutions reaching the highest PPV (≥50 % stenosis: 53.7 % vs. 53.9 % vs. 61.8 % and ≥ 70 % stenosis: 30.4 % vs. 35 % vs. 50 %). Detailed indicators of the diagnostic performance on a per-patient, per-vessel and per-segment basis are presented in Tables S2 and S3.

4. Discussion

This clinical study compared quantitative stenosis measurements based on UHR-CCTA to QCA as a reference. The main results can be summarized as follows: First, UHR-CCTA minimized overestimation bias of quantitative coronary stenosis measurements compared to SR and HR reconstructions, however, still led to significant differences in comparison to QCA. Second, when examining different plaque types, a reduction in overestimation bias was observed only for calcified plaques, but not for non-calcified and partially calcified plaques. Third, diagnostic performance of UHR reconstructions was superior to SR and HR reconstructions for the detection of QCA-confirmed coronary stenosis.

The substantial enhancements in spatial resolution achieved through PCD-CT are particularly relevant for the detection and characterization of CAD, as well as for the advancement of stent patency assessment [15,16]. The recently introduced UHR mode on PCD-CT permits a minimum slice thickness of 0.2 mm, representing a three-fold augmentation in spatial resolution compared to EID imaging.[5] This could present an opportunity to address the issue of overestimating stenosis [17].

Previous phantom studies with PCD-CT were able to show improvements in the visualization of coronary plaques, reduction of stent artifacts, enhanced accuracy in stenosis quantification, and decreased blooming artifacts compared to SR [15,18]. In the present study, median CCTA-measured diameter stenosis decreased with increasing spatial resolution and steadily approached the measured stenosis diameter of the reference method in a study population with a high coronary calcium score. This was also shown by Eberhard et al. who demonstrated

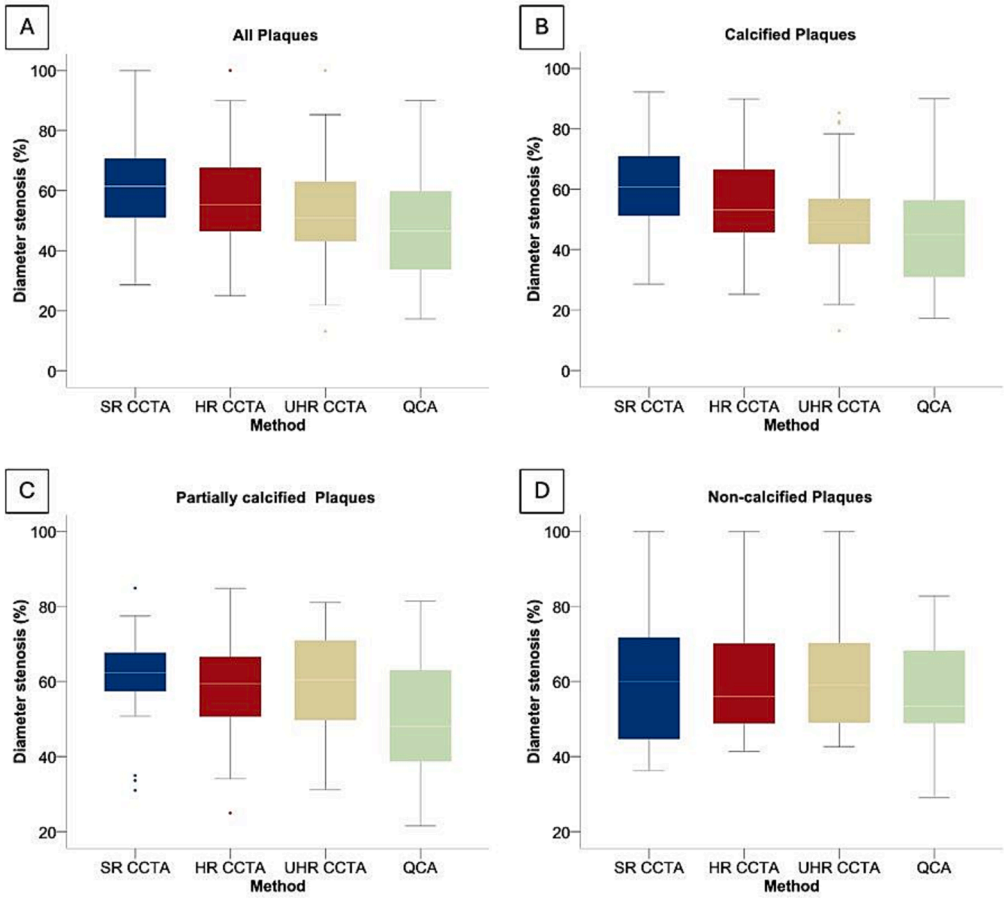

Fig. 2. Diameter stenosis for SR-, HR-, UHR-CCTA, and QCA according to plaque type. (A) All plaques, (B) calcified plaques, (C) partially calcified plaques and (D) non-calcified plaques.

enhanced accuracy in stenosis quantification using UHR compared to invasive QCA in a cohort of 31 patients undergoing transcatheter aortic valve replacement [19]. Patients who had previously undergone stent implantation were not included in this analysis, and as a result, the evaluation of stenosis quantification within stents was not explored. Future research should examine this matter of clinical significance.

Current guidelines recommend CCTA as part of the diagnostic workup for patients suspected of CAD [1,2]. However, its accuracy has limitations, especially in patients with severe calcifications potentially overestimating stenosis severity [4]. Without improved accuracy, especially in populations with high coronary calcium burden, its use could lead to unnecessary additional diagnostic procedures [20]. With the new technology of UHR-CCTA, we were able to demonstrate a significant reduction in bias and LoA, alongside an increasing ICC with higher resolution for calcified plaques. For the assessment of non-calcified and partially calcified plaques, however, these results were not reproducible. The results suggest that the advantage of UHR reconstructions lies mainly in the improved lumen visibility in the presence of calcified plaques. However, in non-calcified and partially calcified plaques there was a subsequent reduction in the LoA with increasing resolution, indicating a narrower spread around the true stenosis diameter determined by QCA, although this did not reach statistical significance. Prior studies have demonstrated that the higher spatial resolution inherently comes at the price of increased image noise which might serve as an explanation for the more difficult delineation of the remaining lumen against the plaque, therefore subsequent overestimation, especially in non-calcified plaques [6]. Enhancements in spectral and spatial resolution are expected to improve characterization of diminutive structures, such as atherosclerotic plaques in coronary arteries [21]. Artificial Intelligence tools have shown promise in reducing image noise for CCTA and chest CT [22,23]. Implementing these tools for CCTA could help evaluate discordance for partially calcified and non-calcified plaques.

The statistical significance between SR and QCA vs. UHR and QCA for partially calcified plaques, but not for HR and QCA, may result from statistical factors. SR and QCA show notably large difference in median stenosis diameter, while comparison of UHR to QCA demonstrates lower measurement variability, contributing to statistical significance. Additionally, SR, with lower spatial resolution and less image noise, and UHR, with higher spatial resolution and more image noise, both offer benefits in plaques with calcified and soft tissue components. HR, with intermediate spatial resolution and image noise, may not be appropriate for accurately assessing stenosis in this specific plaque type. However, this result could also be influenced by the limited number of partially calcified plaques ($n = 20$), requiring cautious interpretation.

With regards on diagnostic accuracy in stenosis quantification over the coronary tree, we observed neither a significant different between proximal and distal coronary nor between the coronary vessels.

Despite the wide clinical use of CCTA, its PPV remains a common limitation. This problem is mainly due to the presence of high calcium burden leading to blooming artifacts, thus a potential overestimation of the diameter stenosis [4,24]. Furthermore, as indicated by the CORE-64 study, CCTA accuracy decreased in patients with high calcium scores [25]. Recently, studies have shown promising results for the improvement of PPV by utilizing the higher spatial resolution of UHR-CCTA [6,7]. However, these studies only provided preliminary evidence as they were either performed in a phantom setting, focused on image quality parameters, or did not include quantitative data in their analysis.

Table 4
Comparison of Stenosis Quantification According to Plaque Types.

		Bland-Altman			
calcified plaques, n = 72[a]	Diameter stenosis (%)	Bias	LoA	ICC	*P* value[b]
CCTA analysis					
SR	60.7 (50.8, 71.2)	15.8	29.6	0.72	<0.001
HR	53.2 (45.6, 67.0)	11.0	28.2	0.76	<0.001
UHR	49.1 (41.8, 57.3)	4.3	23.5	0.84	0.007
QCA reference	44.8 (30.8, 56.7)	n/a			
non-calcified plaques, n = 11					
CCTA analysis					
SR	60.0 (40.5, 72.5)	3.3	20.9	0.91	0.328
HR	56.0 (47.6, 70.5)	3.9	20.5	0.90	0.374
UHR	59.0 (48.2, 72.8)	4.8	19.5	0.91	0.213
QCA reference	53.4 (48.2, 69.8)	n/a			
partially calcified plaques, 20					
CCTA analysis					
SR	62.4 (56.5, 68.4)	9.8	31.0	0.63	0.019
HR	59.4 (50.4, 67.6)	6.8	30.4	0.67	0.073
UHR	60.4 (49.6, 71.2)	8.4	23.2	0.84	0.017
QCA reference	48.1 (37.9, 64.8)	n/a			

LoA, Limits of agreement (1.96 × standard deviation of bias); ICC, intraclass correlation coefficient; CCTA, coronary computed tomography angiography; SR, standard resolution (0.6 mm slice thickness); HR, high resolution (0.4 mm slice thickness); UHR, ultra-high resolution (0.2 mm slice thickness); QCA, quantitative coronary angiography CAD, coronary artery disease.

[a] Number of coronary segments with QCA reference.

[b] Derived from non-parametric pairwise comparison to QCA reference.

Diagnostic accuracy of UHR-CCTA in this analysis was comparable to a recently published study in a high-risk population for CAD in preparation of transcatheter aortic valve replacement which demonstrated high diagnostic accuracy but also low PPV [7]. The slightly lower PPV in our study (PPV 61.8 % for 50 %-stenosis and 50 % for 70 %-stenosis compared to 77 % and 60 %, respectively) may be explained by the forced decision of usage of UHR mode or not, which remains a limitation of the current generation of PCD-CT. In absence of prospective evidence, the choice for or against UHR mode was clinically justified by Agatston scoring, resulting in the exclusion of patients with scores below the chosen cutoff. This may be one of the reasons for the low PPV because the selected cutoff excluded patients with low calcium burden, resulting in a study population with a high Agatston score (median coronary calcium score 993), compared to less than half in the study population investigated by Hagar et al. (414). Importantly, all patients in our cohort received sublingual nitrates and the majority was administered beta-blockers which was not applied in the study by Hagar et al. Another UHR-CCTA study by Kwan et al. with a similar Agatston score (1616) showed comparable values of sensitivity, PPV, NPV and accuracy for the detection of stenoses ≥ 70 % [24]. However, in the per-patient analysis, an increase in PPV for UHR compared to SR and HR was demonstrated for both 50 % and 70 % stenoses, similarly to overall diagnostic accuracy. While this corroboration of prior results is encouraging, the PPV and NPV must be cautiously interpreted in the light of the high prevalence of CAD (45 %, defined as stenosis ≥ 50 %) in the study cohort.

5. Limitations

This study has several limitations. First, the small sample size of 49 patients from a single center, analyzed retrospectively, limits generalizability. Additionally, the 0.6 and 0.4 mm datasets only simulate SR and HR reconstructions based on 0.2 mm PCD raw data, therefore experienced readers might have been able to deduct the type of reconstruction despite our extensive efforts to reduce reading bias. Further, comparison was only performed between measured stenosis diameter from CCTA and QCA, which has several inherent limitations such as dependence on optimal angulations and lacks hemodynamic information. Moreover, exclusion of patients with prior coronary stents further restricts our findings, though investigation of UHR in this population may have future implications. Furthermore, due to the CACS cut-off inclusion criterion resulted in a study sample predominantly composed of calcified plaques, with fewer non-calcified and partially calcified plaques. Consequently, the findings related to these plaque types should be interpreted with caution and warrant further investigation in future studies employing an "all-comer" design. Finally, the comparison of UHR-CCTA and QCA is based on a retrospective analysis and therefore no longitudinal data is accessible, which is essential for examining potential advantages in terms of reducing downstream diagnostics and impacting patient outcomes. Therefore, larger trials investigating clinical endpoints are required to further define the role of UHR-CCTA in clinical practice.

6. Conclusion

UHR-CCTA reconstructions reduced the overestimation bias of coronary stenosis measurements in calcified plaques when evaluated against conventional CCTA using the clinical reference standard QCA. However, there was no diagnostic benefit in non-calcified and partially calcified plaques. Reduced overestimation bias from UHR-CCTA reconstructions, especially in a patient population for which conventional CT scanners have not previously represented a suitable diagnostic tool, has the potential to obviate the need for unnecessary referral for follow-up imaging including ICA. Nevertheless, the limitations of diagnostic quality have not yet been resolved, and further efforts should be made to address this issue.

CRediT authorship contribution statement

Gerald Siegfried Laux: Writing – original draft, Investigation. **Moritz C. Halfmann:** Writing – original draft, Methodology, Investigation. **Larissa Kavermann:** Investigation. **Stefanie Bockius:**

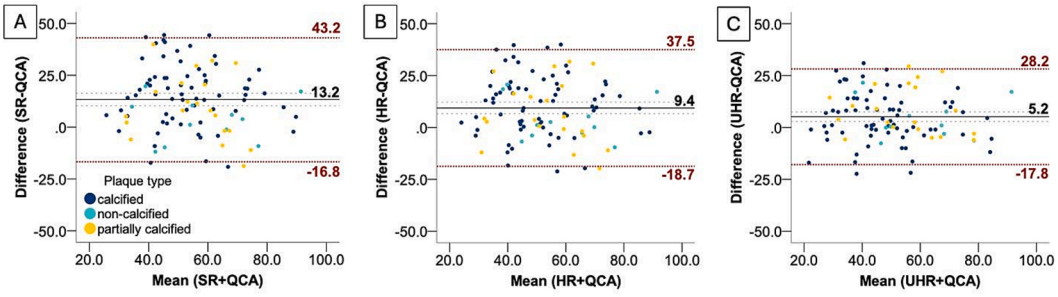

Fig. 3. Bland-Altman plots demonstrate a reduction in overestimation bias of the diameter stenosis as spatial resolution increases. Comparison of quantitative coronary angiography (QCA) to (A) standard resolution (SR), (B) high resolution (HR) and (C) ultra-high resolution (UHR).

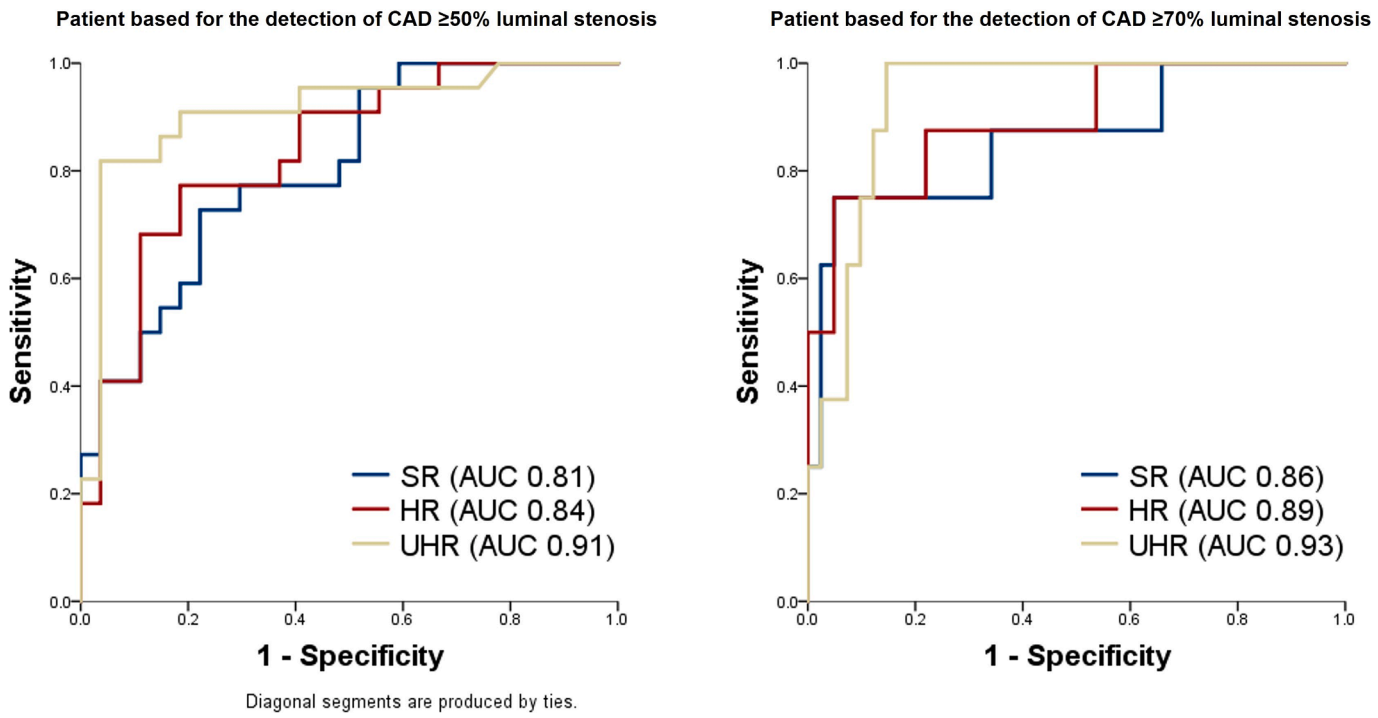

Fig. 4. Receiver operating characteristic (ROC) curves for UHR-CCTA in diagnosing stenosis ≥50% (A) and ≥70% (B) as identified by quantitative coronary angiography.

Investigation. **Maike Knorr:** Investigation. **Tommaso Gori:** Investigation. **Pal Maurovich-Horvat:** Writing – review & editing. **Akos Varga-Szemes:** Writing – review & editing. **Philipp Lurz:** Supervision. **Tobias Bäuerle:** Supervision. **Michaela M. Hell:** Writing – review & editing, Validation, Project administration, Methodology. **Tilman Emrich:** Writing – review & editing, Validation, Project administration, Methodology, Conceptualization.

Funding

This research did not receive any specific grant from funding agencies in the public, commercial, or not-for-profit sectors.

Declaration of competing interest

M. Knorr received speaker's honoraria from Inari Medical, Abbott Cardiovascular, Shockwave Medical, and Boston Scientific. T. Gori received speaker's honoraria from Abbott Cardiovascular, Novartis, Bristol-Myers Squibb, Daiichi Sankyo, Boehringer-Ingelheim, Elixir, SMT, and Pfizer. P. Maurovic-Horvat received speaker's honoraria from Siemens Healthineers and is a shareholder of InterSynk Ltd. A. Varga-Szemes received institutional research and travel support from Siemens Healthineers and is a consultant and shareholder for Elucid Bioimaging. P. Lurz received institutional fees and research grants from Abbott Vascular, Edwards Lifesciences, and ReCor, honoraria from Edwards Lifesciences, Abbott Medical, Innoventric, ReCor, and Boehringer Ingelheim, and has stock options with Innoventric. T. Emrich received speaker's honoraria and travel support and is an advisory board member of Siemens Healthineers and a consultant for Circle Cardiovascular Imaging. M. Halfmann, T. Emrich, and C. Düber report having received institutional research support from Siemens Healthineers. All other authors have no conflicts of interest to declare.

Acknowledgements

This study incorporates aspects of author S.B.'s doctoral thesis.

Appendix A. Supplementary material

Supplementary data to this article can be found online at https://doi.org/10.1016/j.ejrad.2025.112154.

References

[1] F.J. Neumann, U. Sechtem, A.P. Banning, N. Bonaros, H. Bueno, R. Bugiardini, A. Chieffo, F. Crea, M. Czerny, V. Delgado, P. Dendale, J. Knuuti, W. Wijns, F. A. Flachskampf, H. Gohlke, E.L. Grove, S. James, D. Katritsis, U. Landmesser, M. Lettino, C.M. Matter, H. Nathoe, A. Niessner, C. Patrono, A.S. Petronio, S. E. Pettersen, R. Piccolo, M.F. Piepoli, B.A. Popescu, L. Räber, D.J. Richter, M. Roffi, F.X. Roithinger, E. Shlyakhto, D. Sibbing, S. Silber, I.A. Simpson, M. Sousa-Uva, P. Vardas, A. Witkowski, J.L. Zamorano, S. Achenbach, S. Agewall, E. Barbato, J. J. Bax, D. Capodanno, T. Cuisset, C. Deaton, K. Dickstein, T. Edvardsen, J. Escaned, C. Funck-Brentano, B.J. Gersh, M. Gilard, D. Hasdai, R. Hatala, F. Mahfoud, J. Masip, C. Muneretto, E. Prescott, A. Saraste, R.F. Storey, P. Svitil, M. Valgimigli, V. Aboyans, C. Baigent, J.P. Collet, V. Dean, D. Fitzsimons, C.P. Gale, D.E. Grobbee, S. Halvorsen, G. Hindricks, B. Iung, P. Jüni, H.A. Katus, C. Leclercq, B.S. Lewis, B. Merkely, C. Mueller, S. Petersen, R.M. Touyz, S. Benkhedda, B. Metzler, V. Sujayeva, B. Cosyns, Z. Kusljugic, V. Velchev, G. Panayi, P. Kala, S.A. Haahr-Pedersen, H. Kabil, T. Ainla, T. Kaukonen, G. Cayla, Z. Pagava, J. Woehrle, J. Kanakakis, K. Toth, T. Gudnason, A. Peace, D. Aronson, C. Riccio, S. Elezi, E. Mirrakhimov, S. Hansone, A. Sarkis, R. Babarskiene, J. Beissel, A.J. Cassar Maempel, V. Revenco, G.J. de Grooth, H. Pejkov, V. Juliebø, P. Lipiec, J. Santos, O. Chioncel, D. Duplyakov, L. Bertelli, A.D. Dikic, M. Studencan, M. Bunc, F. Alfonso, M. Back, M. Zellweger, F. Addad, A. Yildirir, Y. Sirenko, B. Clapp, ESC Guidelines for the diagnosis and management of chronic coronary syndromes, Eur Heart J 41 (2020) (2019) 407–477, https://doi.org/10.1093/eurheartj/ehz425.

[2] M. Gulati, P.D. Levy, D. Mukherjee, E. Amsterdam, D.L. Bhatt, K.K. Birtcher, R. Blankstein, J. Boyd, R.P. Bullock-Palmer, T. Conejo, D.B. Diercks, F. Gentile, J. P. Greenwood, E.P. Hess, S.M. Hollenberg, W.A. Jaber, H. Jneid, J.A. Joglar, D. A. Morrow, R.E. O'Connor, M.A. Ross, L.J. Shaw, AHA/ACC/ASE/CHEST/SAEM/SCCT/ SCMR guideline for the evaluation and diagnosis of chest pain: a report of the American college of cardiology/American heart association joint committee on clinical practice guidelines, Circulation 144 (2021) (2021) E368–E454, https://doi.org/10.1161/CIR.0000000000001029.

[3] A.J. Moss, M.C. Williams, D.E. Newby, E.D. Nicol, The updated NICE guidelines: cardiac CT as the first-line test for coronary artery disease, Curr Cardiovasc Imaging Rep 10 (2017), https://doi.org/10.1007/s12410-017-9412-6.

[4] A.L. Vavere, A. Arbab-Zadeh, C.E. Rochitte, M. Dewey, H. Niinuma, I. Gottlieb, M. E. Clouse, D.E. Bush, J.W.M. Hoe, A. De Roos, C. Cox, J.A.C. Lima, J.M. Miller, Coronary artery stenoses: accuracy of 64-detector row CT angiography in segments with mild, moderate, or severe calcifi cation-a subanalysis of the CORE-64 trial 1, Radiology.rsna.org n Radiology 261 (2011), https://doi.org/10.1148/radiol.11110537/-/DC1.

[5] M.J. Willemink, M. Persson, A. Pourmorteza, N.J. Pelc, D. Fleischmann, Photon-counting CT: technical principles and clinical prospects, Radiology 289 (2018) 293–312, https://doi.org/10.1148/radiol.2018172656.
[6] V. Mergen, T. Sartoretti, M. Baer-Beck, B. Schmidt, M. Petersilka, J.E. Wildberger, A. Euler, M. Eberhard, H. Alkadhi, Ultra-high-resolution coronary CT angiography with photon-counting detector CT: feasibility and image characterization, Invest Radiol 57 (2022) 780–788, https://doi.org/10.1097/RLI.0000000000000897.
[7] M.T. Hagar, M. Soschynski, R. Saffar, A. Rau, J. Taron, J. Weiss, T. Stein, S. Faby, C. von Zur Muehlen, P. Ruile, C.L. Schlett, Accuracy of ultrahigh-resolution photon-counting CT for detecting coronary artery disease in a high-risk population, Radiology 307 (2023), https://doi.org/10.1148/radiol.223305.
[8] V. Mergen, M. Eberhard, R. Manka, A. Euler, H. Alkadhi, First in-human quantitative plaque characterization with ultra-high resolution coronary photon-counting CT angiography, Front Cardiovasc Med 9 (2022), https://doi.org/10.3389/fcvm.2022.981012.
[9] S. Trattner, S. Halliburton, C.M. Thompson, Y. Xu, A. Chelliah, S.R. Jambawalikar, B. Peng, M.R. Peters, J.E. Jacobs, M. Ghesani, J.J. Jang, H. Al-Khalidi, A.J. Einstein, Cardiac-specific conversion factors to estimate radiation effective dose from dose-length product in computed tomography, JACC Cardiovasc Imaging 11 (2018) 64–74, https://doi.org/10.1016/j.jcmg.2017.06.006.
[10] V. Cheng, A. Gutstein, A. Wolak, Y. Suzuki, D. Dey, H. Gransar, L.E. J Thomson, S. W. Hayes, J.D. Friedman, D.S. Berman, Moving Beyond Binary Grading of Coronary Arterial Stenoses on Coronary Computed Tomographic Angiography Insights for the Imager and Referring Clinician, 2008. https://doi.org/10.1016/j.jcmg.2008.05.006.
[11] J. Leipsic, S. Abbara, S. Achenbach, R. Cury, J.P. Earls, G.B.J. Mancini, K. Nieman, G. Pontone, G.L. Raff, SCCT guidelines for the interpretation and reporting of coronary CT angiography: a report of the society of cardiovascular computed tomography guidelines committee, J Cardiovasc Comput Tomogr 8 (2014) 342–358, https://doi.org/10.1016/j.jcct.2014.07.003.
[12] L. Koweek, S. Achenbach, D.S. Berman, J.J. Carr, R.C. Cury, B. Ghoshhajra, D. Litmanovich, C.H. McCollough, A.J. Taylor, Q.A. Truong, J. Wang, W. G. Weigold, A. Arbab-Zadeh, S. Abbara, M.Y. Chen, Standardized medical terminology for cardiac computed tomography 2023 update, J Cardiovasc Comput Tomogr 17 (2023) 345–354, https://doi.org/10.1016/j.jcct.2023.06.002.
[13] N. Suzuki, T. Asano, G. Nakazawa, J. Aoki, K. Tanabe, K. Hibi, Y. Ikari, K. Kozuma, Clinical expert consensus document on quantitative coronary angiography from the Japanese Association of Cardiovascular Intervention and Therapeutics, Cardiovasc Interv Ther 35 (2020) 105–116, https://doi.org/10.1007/s12928-020-00653-7.
[14] T.K. Koo, M.Y. Li, A Guideline of selecting and reporting intraclass correlation coefficients for reliability research, J Chiropr Med 15 (2016) 155–163, https://doi.org/10.1016/j.jcm.2016.02.012.
[15] J.R. Rajagopal, F. Farhadi, T. Richards, M. Nikpanah, P. Sahbaee, S.M. Shanbhag, W. Patricia Bandettini, B. Saboury, A.A. Malayeri, W.F. Pritchard, E.C. Jones, E. Samei, M.Y. Chen, Evaluation of coronary plaques and stents with conventional and photon-counting ct: benefits of highresolution photon-counting ct, Radiol Cardiothorac Imaging 3 (2021), https://doi.org/10.1148/ryct.2021210102.
[16] S.A. Si-Mohamed, S. Boccalini, H. Lacombe, A. Diaw, M. Varasteh, P.A. Rodesch, R. Dessouky, M. Villien, V. Tatard-Leitman, T. Bochaton, P. Coulon, Y. Yagil, E. Lahoud, K. Erhard, B. Riche, E. Bonnefoy, G. Rioufol, G. Finet, C. Bergerot, L. Boussel, J. Greffier, P.C. Douek, Coronary CT angiography with photon-counting CT: first-in-human results, Radiology 303 (2022) 303–313, https://doi.org/10.1148/RADIOL.211780.
[17] J. Latina, M. Shabani, K. Kapoor, S.P. Whelton, J.C. Trost, J. Sesso, S. Demehri, M. Mahesh, J.A.C. Lima, A. Arbab-Zadeh, Ultra-high-resolution coronary ct angiography for assessment of patients with severe coronary artery calcification: initial experience, Radiol Cardiothorac Imaging 3 (2021), https://doi.org/10.1148/ryct.2021210053.
[18] E. Zsarnoczay, N. Fink, U.J. Schoepf, J. O'Doherty, T. Allmendinger, J. Hagenauer, E.V. Wolf, J.P. Griffith, P. Maurovich-Horvat, A. Varga-Szemes, T. Emrich, Ultra-high resolution photon-counting coronary CT angiography improves coronary stenosis quantification over a wide range of heart rates – a dynamic phantom study, Eur J Radiol 161 (2023), https://doi.org/10.1016/j.ejrad.2023.110746.
[19] M. Eberhard, A. Candreva, R. Rajagopal, V. Mergen, T. Sartoretti, B.E. Stähli, C. Templin, R. Manka, H. Alkadhi, Coronary stenosis quantification with ultra-high-resolution photon-counting detector CT angiography: comparison with 3D quantitative coronary angiography, JACC Cardiovasc Imaging (2023), https://doi.org/10.1016/j.jcmg.2023.10.004.
[20] J. Simon, Á. Hrenkó, N.M. Kerkovits, K. Nagy, M. Vértes, H. Balogh, N. Nagy, T. Munkácsi, T. Emrich, A. Varga-Szemes, M. Boussoussou, B. Vattay, M. Vecsey-Nagy, M. Kolossváry, B. Szilveszter, B. Merkely, P. Maurovich-Horvat, Photon-counting detector CT reduces the rate of referrals to invasive coronary angiography as compared to CT with whole heart coverage energy-integrating detector, J Cardiovasc Comput Tomogr 18 (2024) 69–74, https://doi.org/10.1016/j.jcct.2023.11.079.
[21] P.C. Douek, S. Boccalini, E.H.G. Oei, D.P. Cormode, A. Pourmorteza, L. Boussel, S. A. Si-Mohamed, R.P.J. Budde, Clinical applications of photon-counting CT: a review of pioneer studies and a glimpse into the future, Radiology 309 (2023), https://doi.org/10.1148/radiol.222432.
[22] B. Jiang, N. Li, X. Shi, S. Zhang, J. Li, G.H. de Bock, R. Vliegenthart, X. Xie, Deep learning reconstruction shows better lung nodule detection for ultra–low-dose chest CT, Radiology 303 (2022) 202–212, https://doi.org/10.1148/RADIOL.210551.
[23] S. Chang, N.R. Huber, J.F. Marsh, E.K. Koons, H. Gong, L. Yu, C.H. McCollough, S. Leng, Pie-net: prior-information-enabled deep learning noise reduction for coronary CT angiography acquired with a photon counting detector CT, Med Phys 50 (2023) 6283–6295, https://doi.org/10.1002/mp.16411.
[24] A.C. Kwan, H. Gransar, E. Tzolos, B. Chen, Y. Otaki, E. Klein, A.J. Pope, D. Han, A. Howarth, N. Jain, D. Dey, R.J. Miller, V. Cheng, B. Azarbal, D.S. Berman, The accuracy of coronary CT angiography in patients with coronary calcium score above 1000 Agatston Units: Comparison with quantitative coronary angiography: coronary CT angiography in high coronary calcium, J Cardiovasc Comput Tomogr 15 (2021) 412–418, https://doi.org/10.1016/j.jcct.2021.03.007.
[25] A. Arbab-Zadeh, J.M. Miller, C.E. Rochitte, M. Dewey, H. Niinuma, I. Gottlieb, N. Paul, M.E. Clouse, E.P. Shapiro, J. Hoe, A.C. Lardo, D.E. Bush, A. De Roos, C. Cox, J. Brinker, J.A.C. Lima, Diagnostic accuracy of computed tomography coronary angiography according to pre-test probability of coronary artery disease and severity of coronary arterial calcification: The CORE-64 (Coronary Artery Evaluation Using 64-Row Multidetector Computed Tomography Angiography) international multicenter study, J Am Coll Cardiol 59 (2012) 379–387, https://doi.org/10.1016/j.jacc.2011.06.079.